

Photoelectric effects of ultraviolet fast response and high sensitivity in LiNbO_3 single crystal

Er-Jia Guo,¹ Jie Xing,^{1,2} Kui-Juan Jin,¹ Hui-Bin Lu,^{1,a)} Juan Wen,¹ and Guo-Zhen Yang¹

¹Beijing National Laboratory for Condensed Matter Physics, Institute of Physics, Chinese Academy of Science, Beijing 100190, People's Republic of China

²School of Materials Sciences and Technology, China University of Geosciences, Beijing 100083, People's Republic of China

(Received 17 April 2009; accepted 24 June 2009; published online 29 July 2009)

The photoelectric effects in LiNbO_3 (LNO) single crystal have been systematically studied with the two kinds of LNO wafers of tilt of 10° and untilted at the ambient temperature. The ultrafast response photoelectric effect of 120 ps rise time was observed in 10° tilted LNO single crystal with a 266 nm laser pulse of 25 ps duration. The photocurrent responsivity of untilted LNO with an interdigitated electrode of 10 μm finger width and 10 μm interspacing is 17.1 mA/W under the irradiation of 300 nm wavelength UV light at 10 V bias. The noise current under sunlight is only 73 pA at 10 V bias. The experimental results suggest that the LNO single crystal is one of the promising materials for photodetectors working in UV region. © 2009 American Institute of Physics.

[DOI: 10.1063/1.3183957]

I. INTRODUCTION

Lithium niobate (LiNbO_3 , LNO) single crystal, one of the perovskite-type oxide materials, has many excellent properties, such as ferroelectric effect, Pockels effect, piezoelectric effect, photoelasticity, and nonlinear optical polarizability.¹⁻⁵ Over the years, LNO single crystals are widely used in manufacturing surface acoustic wave devices and frequency converters due to its high electromechanical coupling coefficients and large electro-optic coefficients,^{6,7} as well as in waveguide fabrication for optical information process, communicate, and storage technology.⁸⁻¹⁰ We reported the ultraviolet (UV) photoelectric effects in SrTiO_3 and LaAlO_3 single crystals,¹¹⁻¹³ and also the visible-blind SrTiO_3 UV photodetector.¹⁴ Similar to SrTiO_3 and LaAlO_3 , the bandgap of LNO single crystal is ~ 4 eV,¹⁵ corresponding to a bandgap excitation of ~ 310 nm wavelength and suggesting that LNO single crystal is a promising material for photodetector working in UV region. However, as far as we know, the UV photodetector based on LNO single crystal has not been reported yet. In this letter, we report the UV ultrafast photoelectric effects in LNO single crystal and prove the potential application of LNO single crystal in UV detection.

II. EXPERIMENTS

The LNO wafers used in the present study are as-supplied LNO (001) single crystal wafers with the purity of 99.99% and mirror single polished. The geometry size of all the LNO wafers is 5×10 mm² with a thickness of 0.5 mm. In order to investigate the photoelectric effects of LNO single crystal and its application in UV detection, two kinds of LNO wafers of tilt of 10° and untilted were used in the experiments. To prevent the influences of external electrical

field, we choose the 10° tilted LNO wafer to study the photoelectric effect by measuring the open-circuit photovoltage. As shown in Fig. 1(a), the (001) plane of tilted LNO wafers is miscut as an angle of 10° with respect to the (110) plane. The tilting of the c axis was further confirmed by an x-ray diffraction measurement with the $\theta \sim 2\theta$ scan. Two indium electrodes were painted on the polished surface of 10° tilted LNO wafers and separated by 1 mm. Thus, the efficient area

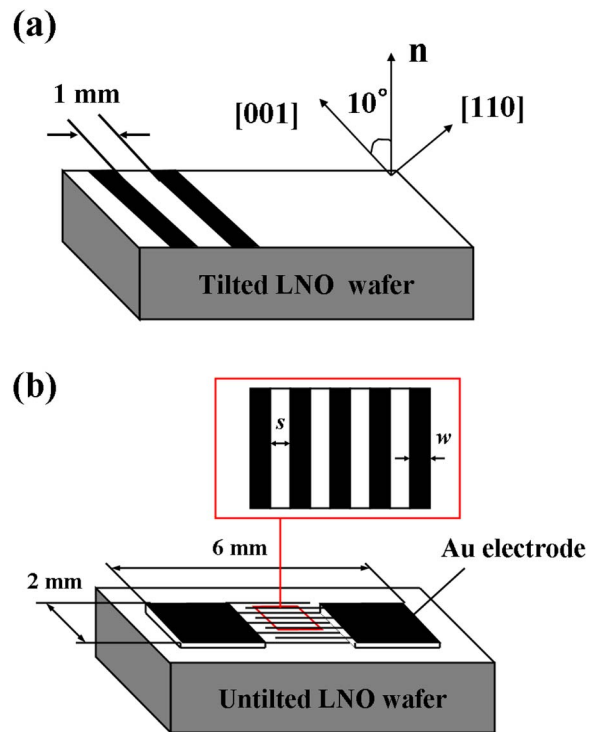


FIG. 1. (Color online) (a) Schematic diagram of tilted LNO wafer and the electrodes structure. The LNO (001) plane is tilted to the surface of the wafer with an angle of 10° . (b) Schematic diagram of the interdigitated electrodes configuration on untilted LNO (001) surface, where w and s represent the width and interspacing of the electrodes and $w=s$.

^{a)}Author to whom correspondence should be addressed. Electronic mail: hblu@aphy.iphy.ac.cn.

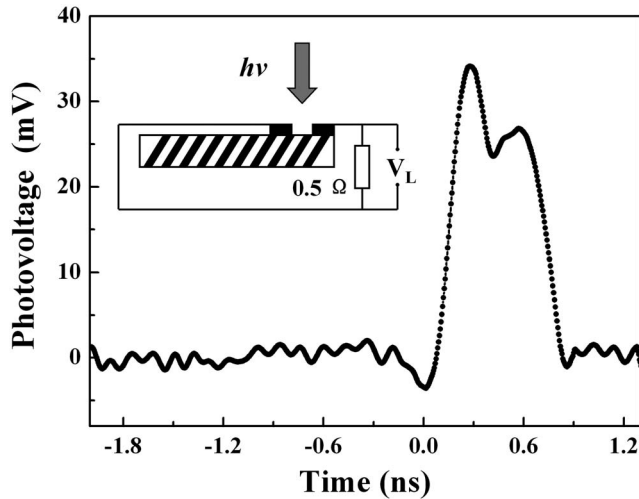


FIG. 2. A typical transient open-circuit photoelectric signal of tilted 10° LNO under an excitation of a 266 nm laser pulse of 25 ps duration and measured by oscilloscope with $1\text{ M}\Omega$ impedance. The LNO wafer is connected in parallel with a $0.5\ \Omega$ resistance. The inset shows the schematic circuit of the measurement.

is $1 \times 5\text{ mm}^2$. A fourth harmonic of an actively passively mode-locked Nd:YAG (yttrium aluminum garnet) laser (266 nm, 25 ps, and $12.7\ \mu\text{J}/\text{mm}^2$) was chosen as the light source and the energy on the effective area of LNO wafer was $63.5\ \mu\text{J}$. The photoelectric signals were recorded by a 2.5 GHz bandwidth sampling oscilloscope (Tektronix TDS7254B).

The untilted LNO wafer was used to study the application in UV detection. As shown in the Fig. 1(b), a Au layer with thickness of 100 nm was deposited onto the polished surface of LNO wafers by electron-gun evaporation. Conventional UV lithography and etching were performed to fabricate the Au interdigitated electrodes. The effective area of the photodetector is $2 \times 6\text{ mm}^2$. The finger width w and the interspacing s of the electrodes have the same size of $10\ \mu\text{m}$. A dc voltage source was taken as supplied bias. A monochromatic Hg lamp (253.65 nm, $0.53\text{ mW}/\text{cm}^2$) and the Nd:YAG pulsed laser mentioned above were employed as the light sources. The spectral responsivity was measured by a monochromator with a standard lock-in amplifier. A 30 W D_2 lamp was used as the light source. We measured the noise current under sunlight by using a Keithley model 2182 nanovoltmeter. The powers of Hg and D_2 lamps have been calibrated by a UV-enhanced silicon photodetector.

III. RESULTS AND DISCUSSION

Figure 2 shows a typical transient open-circuit photovoltaic signal when a 266 nm laser pulse is irradiated directly onto the 10° tilted LNO surface. The schematic of the measurement circuit is shown in the inset of Fig. 2. To reduce the RC influence in the measurement circuit, we connected a $0.5\ \Omega$ resistance in parallel with LNO wafer as shown in the inset of Fig. 2. The rise time (10%–90%) of the photoelectric signal is 120 ps and the full width at half maximum (FWHM) is 557 ps, indicating that the photovoltage in LNO single crystal is an ultrafast process.

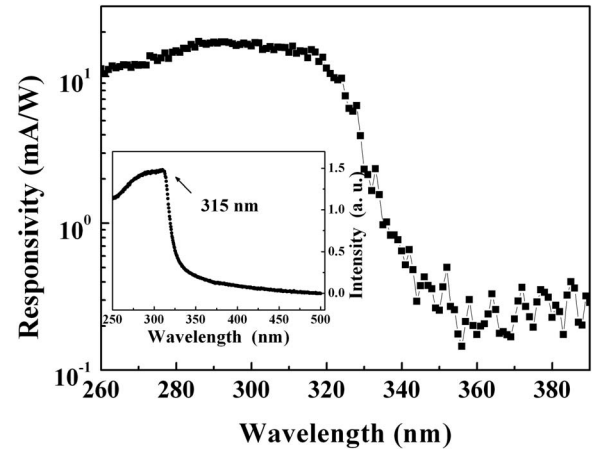


FIG. 3. The spectral response of untilted LNO wafer with $10\ \mu\text{m}$ width and $10\ \mu\text{m}$ interspacing interdigitated electrodes at 10 V bias. The absorption spectra of LNO single crystal are shown in the inset.

The mechanism of photovoltage in tilted LNO wafer, similar to SrTiO_3 single crystal,^{11,12} can be understood as following: LNO single crystal absorbed the induced photons and generated the carriers (electron and hole) as well as a thermal gradient field. According to thermoelectric theory, the lateral thermoelectric field $E(x) = (S_{ab} - S_c) \sin 2\alpha (dT/dz)/2$, where S_{ab} and S_c are the Seebeck coefficients of the LNO crystal along the ab plane and c axis, α is the vicinal cut angle, and dT/dz denotes the temperature gradient in the direction of irradiation (perpendicular to surface).¹⁶ The thermoelectric field leads to the separation of the photocarriers in the lateral direction and resulted in the photovoltage between the two electrodes. From the thermoelectric formula, we can see that the lateral photovoltage has a sinusoidal relationship with the tilted angle α . When α is zero, no lateral field can be built and no photovoltage can be observed in lateral direction, which is in agreement with our experimental results. The polarity of photovoltage is reversed when the laser incidence from back side of LNO wafer because the direction of temperature gradient in the LNO (001) is reversal. As mentioned above, the photovoltage in tilted LNO is a combinational process of photoelectric effect and thermoelectric effect.

The inset in Fig. 3 shows the absorption spectra of LNO single crystal we measured at ambient temperature. The absorption peak and the absorption edge appear at about 315 and 330 nm, respectively, corresponding to an optical bandgap of $\sim 3.8\text{ eV}$. The bandgap of 3.8 eV is a little smaller than 4 eV as usual.¹⁵ The reason for causing the difference of bandgap may be that the LNO single crystals were fabricated by different preparation processes. Figure 3 displays the spectral response of the LNO with $10\ \mu\text{m}$ interdigitated electrodes at 10 V bias measured by a monochromator with a 30 W D_2 lamp. The photocurrent responsivity is $17.1\text{ mA}/\text{W}$ at 300 nm wavelength. The UV/visible (300 versus 390 nm) contrast ratio is more than two orders of magnitude. The cutoff wavelength appears at about 330 nm, which is in agreement with the absorption spectra of LNO single crystal. The cutoff wavelength corresponds to the energy of 3.8 eV, demonstrating a bandgap excitation process.

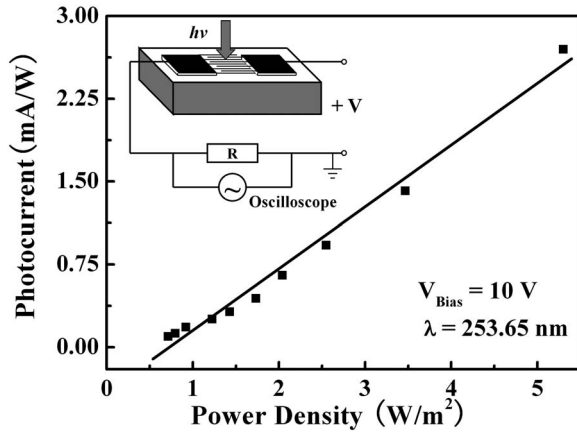


FIG. 4. The photocurrent responsivity of unilted LNO wafer varies with the power density of Hg lamp. The sample is in series with a sampling resistance $R=1\text{ M}\Omega$ and measured at 10 V bias. The inset displays the schematic circuit of measurement. The solid line presented in the figure is a guide for eyes.

Based on the ultrafast photoelectrical effect of the LNO single crystal mentioned above, we further studied the application of LNO single crystal in UV detection with interdigitated electrodes as shown in Fig. 1(b) under external bias. Figure 4 exhibits the photocurrent responsivity as a function of the power density of incident light with the LNO of $10\text{ }\mu\text{m}$ interdigitated electrodes under 253.65 nm irradiation at 10 V bias. The schematic of the measurement circuit is shown in the inset of Fig. 4. A sampling resistance $R=1\text{ M}\Omega$ was in series with the LNO wafer, the photocurrents were calculated by $I_L=V_L/R$, where V_L is the voltages across the sampling resistance R . We can see that the magnitude of photocurrent responsivity increased linearly with the power density of incident light.

Figure 5 exhibits the bias dependence of the photocurrent responsivity under 253.65 nm irradiation for the LNO wafer with $10\text{ }\mu\text{m}$ interdigitated electrodes. The magnitude of photocurrent responsivity also increased linearly with the applied bias. The inset in Fig. 5 shows the variation in noise current with the applied bias. We measured the noise current

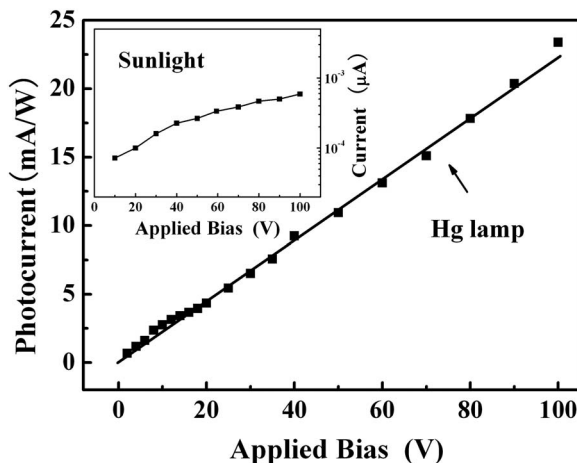


FIG. 5. The bias dependence of photocurrent responsivity in unilted LNO under Hg lamp illumination. The inset shows a semilog scale of the variation in noise current with the bias which was measured under sunlight illumination. The solid line presented in the figure is a guide for eyes.

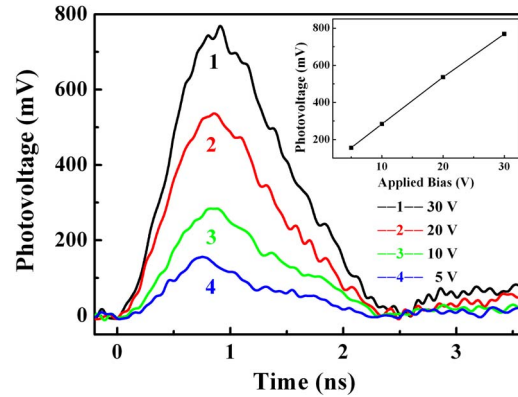


FIG. 6. (Color online) Transient photoresponses of unilted LNO under the excitation of 266 nm pulsed laser with 25 ps duration at 5, 10, 20, and 30 V biases, respectively. A $0.5\text{ }\Omega$ resistance connected in parallel with the LNO wafer and photovoltages were measured by a 2.5 GHz bandwidth oscilloscope. The inset shows the bias dependence of photovoltages under 266 nm pulsed laser illumination.

directly under the illumination of sunlight at mid-day in outdoor. The noise currents under sunlight irradiation are 73, 264, and 588 pA at 10, 50, and 100 V biases, respectively. Compare with the photocurrent responsivity in Fig. 5, the signal to noise ratio is more than two orders of magnitude, suggesting the potential application of LNO detector to detect DUV ($<290\text{ nm}$) directly without any filters to block the sunlight.

We also measured the transient responses of LNO with interdigitated electrodes under the same experimental conditions with measuring the 10° tilted LNO in Fig. 2. A $0.5\text{ }\Omega$ resistance was connected in parallel with LNO wafer which was irradiated by 266 nm pulsed laser; Fig. 6 shows the transient responses of LNO with interdigitated electrodes under different biases. The photovoltages are also linearly dependent on the bias as shown in the inset of Fig. 6. The rise time and FWHM are about 500 ps and 1 ns for the different biases, respectively, demonstrating that the devices we made were also ultrafast response to the UV light. The photovoltages are 156, 284, 536, and 769 mV at 5, 10, 20, and 30 V biases, respectively. Compare with the result in Fig. 2, at the same bias of 10 V, the photovoltaic sensitivity in Fig. 6 is eight times higher than that in Fig. 2. The sensitivity was much improved because the recombination of photogenerated carriers can be reduced and more carriers can be collected by using the interdigitated electrodes and external bias.

IV. SUMMARY

In conclusion, we studied the UV photoelectric effects in LNO single crystal with the two kinds LNO wafers of tilt of 10° and unilted. The ultrafast response photoelectric effect of 120 ps rise time was observed in 10° tilted LNO single crystal. The LNO device with $10\text{ }\mu\text{m}$ interdigitated electrodes showed the high signal to noise ratio, good linear dependence to the bias, and high sensitivity. The photocurrent responsivity reached 17.1 mA/W under the irradiation of 300 nm wavelength at 10 V bias. The UV/visible (300 versus 390 nm) contrast ratio is more than two orders of the mag-

nitide. The noise current under sunlight is only 73 pA at 10 V bias. The experimental results proved that the LNO single crystal is a promising material for photodetectors working in UV region. Especially, the LNO is based on commercial LNO single crystal and do not need complex fabrication process, suggesting a broad potential application in the fields of military and civilian.

ACKNOWLEDGMENTS

This work is supported by the National Natural Science Foundation of China and the National Basic Research Program of China.

¹A. Fiore, V. Berger, E. Rosencher, P. Bravetti, and J. Nagle, *Nature (London)* **391**, 463 (1998).

²I. Inbar and R. E. Cohen, *Phys. Rev. B* **53**, 1193 (1996).

³S. Çabuk and A. Mamedov, *J. Opt. A, Pure Appl. Opt.* **1**, 424 (1999).

⁴K. Wang, J. F. Li, and N. Liu, *Appl. Phys. Lett.* **93**, 092904 (2008).

⁵T. Ellenbogen, I. Dolev, and A. Arie, *Opt. Lett.* **33**, 1207 (2008).

⁶Y. Shibata, K. Kaya, K. Akashi, M. Kanai, T. Kawai, and S. Kawai, *Appl. Phys. Lett.* **61**, 1000 (1992).

⁷P. Baldi, M. P. D. Micheli, K. E. Hadi, S. Nouh, and A. C. Cino, *Opt. Eng. (Bellingham)* **37**, 1193 (1998).

⁸R. R. Thomson, S. Campbell, I. J. Blewett, A. K. Kar, and D. T. Reid, *Appl. Phys. Lett.* **88**, 111109 (2006).

⁹J. Burghoff, H. Hartung, S. Nolte, and A. Tünnermann, *Appl. Phys. A: Mater. Sci. Process.* **86**, 165 (2007).

¹⁰X. L. Zeng, X. F. Chen, Y. P. Chen, Y. X. Xia, and Y. L. Chen, *Opt. Laser Technol.* **35**, 187 (2003).

¹¹K. Zhao, K. J. Jin, Y. H. Huang, S. Q. Zhao, H. B. Lu, M. He, Z. H. Chen, Y. L. Zhou, and G. Z. Yang, *Appl. Phys. Lett.* **89**, 173507 (2006).

¹²K. Zhao, H. B. Lu, and M. He, *Eur. Phys. J.: Appl. Phys.* **41**, 139 (2008).

¹³X. Wang, J. Xing, K. Zhao, J. Li, Y. H. Huang, K. J. Jin, M. He, H. B. Lu, and G. Z. Yang, *Physica B* **392**, 104 (2007).

¹⁴J. Xing, K. Zhao, H. B. Lu, X. Wang, G. Z. Liu, K. J. Jin, M. He, C. C. Wang, and G. Z. Yang, *Opt. Lett.* **32**, 2526 (2007).

¹⁵V. Tatyana and W. Manfred, *Lithium Niobate: Defects, Photorefractive and Ferroelectric Switching* (Springer, Berlin, 2008), pp. 1–9.

¹⁶H. Lengfellner, G. Kremb, A. Schnellbögl, J. Betz, K. F. Renk, and W. Prettl, *Appl. Phys. Lett.* **60**, 501 (1992).